New SOS Diode Pumping Circuit Based on an All-Solid-State Spiral Generator for High-Voltage Nanosecond Applications

Anton I. Gusev, *Member, IEEE,* Ivan Lavrinovich, *Member, IEEE,* Antoine Silvestre de Ferron, Laurent Pecastaing, *Senior Member, IEEE,* Simon Bland, *Member, IEEE,* Susan Parker, Jiaqi Yan, *Associate Member, IEEE,* and Bucur M. Novac, *Senior Member, IEEE*

***Abstract*—Semiconductor opening switch (SOS) diodes are capable to switch currents with a density of more than 1 kA/cm² and withstand nanosecond pulses with an amplitude of up to 1 MV. SOS diodes however require a specific pumping circuit that must simultaneously provide forward and reverse pumping currents with a time of ~500 ns and ~100 ns, respectively. Such a pumping circuit with energies > 1 J typically requires a gas-discharge switch or a low-efficient solid-state solution. This study proposes a novel approach to pumping SOS diodes based on a spiral generator (a.k.a. vector inversion generator). Due to its wave characteristics, the spiral generator produces a bipolar current discharge that meets the time duration and current amplitude required to pump an SOS diode. Moreover, the initial pulse from the spiral typically has a relatively low current amplitude compared to the opposite polarity secondary pulse – so the SOS diode can operate at very high efficiencies. This idea has been tested using an all-solid-state spiral generator coupled with large-area SOS diodes (1 cm²). With this combination, a voltage pulse of 62 kV having a rise time of only 11 ns was obtained on an open circuit load (3 pF, 1 MΩ). The experiments were highly repeatable, with no damage to the components despite multiple tests. There is significant scope to further improve the results, with simple alterations to the spiral generator.**

***Index Terms*—Pulsed power systems, semiconductor opening switches, solid-state circuits, spiral generators.**

Manuscript received 31 December 2022; revised X Xxxx 2023; accepted XX Xxxxx 2023. Date of publication XX Xxxx 2023; date of current version XX Xxxxxx 2023. This work was supported in part by the "Investissements d'Avenir" French Program under the framework of Energy and Environment Solutions (E2S) Université de Pau et des Pays de l'Adour (UPPA) (Solid-State Pulsed Power (S2P2) Chair and Pulsed Power Applications (PULPA) Chair) managed by Agence Nationale de la Recherche (ANR) under Grant ANR-16-IDEX-0002 and in part by the Imperial College Engineering and Physical Sciences Research Council (EPSRC) Impact Acceleration Account. The review of this article was arranged by Senior Editor X. X. Xxxxx. (*Corresponding author: Anton I. Gusev.*)

Anton I. Gusev, Ivan Lavrinovich, Antoine Silvestre de Ferron, and Laurent Pecastaing are with the Laboratoire SIAME, Equipe Procédés Haute Tension, Université de Pau et des Pays de l'Adour, 64053 Pau, France (e-mail: anton.gusev@univ-pau.fr).

Simon Bland, Susan Parker, and Jiaqi Yan are with the Department of Physics, Faculty of Natural Sciences, Imperial College London, London SW7 2BX, U.K. (e-mail: sn.bland@imperial.ac.uk).

Bucur M. Novac is with the Wolfson School of Mechanical, Electrical and Manufacturing Engineering, Loughborough University, Loughborough LE11 3TU, U.K. (e-mail: b.m.novac@lboro.ac.uk).

Color versions of one or more figures in this article are available at https://doi.org/10.1109/TPS.2023.XXXXXXX.

Digital Object Identifier 10.1109/TPS.2023.XXXXXXX

I. INTRODUCTION

SOLID-STATE pulsed power is attracting more and more attention due to its distinct advantages over traditional gas-discharge methods of generating nanosecond, high-voltage electrical pulses. Semiconductor switches are free of gas-discharge switch weaknesses such as electrode erosion, dielectric contamination, and jitter. Therefore, solid-state pulsed power systems with their long lifetime and high average power find numerous industrial applications in medicine, agriculture, food processing, etc.

Drift step recovery diodes (DSRD) [1] and semiconductor opening switch diodes (SOS) [2] are one of the most powerful semiconductor switches up to date. They operate as follows. First, the submicrosecond forward current injects electron-hole plasma into the diode structure. This process is referred to as "forward pumping". Then, current flows through the diodes in a reverse direction, storing energy in inductive energy storage. This phase is called "reverse pumping". Finally, diodes cut off the current, forming a high-voltage nanosecond pulse across the load.

Both DSRD and SOS diodes work similarly in terms of circuit design, yet completely different in terms of physics. According to a comparison of DSRD and SOS diodes [3], the current cut-off occurs at the p-n junction for DSRD and at the p region for SOS. This difference in operation eventually results in different ultimate parameters of cut-off current density and peak power: 10^2 A/cm², 10^8 W for DSRD and 10^5 A/cm², 10^{10} W for SOS [3]. Due to extremely high peak power, SOS diodes are employed in many pulsed power applications, as described in the comprehensive review of the SOS technology in [4]. It includes electron accelerators, X-ray pulse devices, high-power microwave electronics, pumping of gas lasers, and ignition of electrical discharges.

However, a pumping circuit of the SOS diode is challenging since it has to generate a forward current of 100 A / 500 ns and a reverse current of 1 kA / 100 ns. To keep the all-solid-state approach, several energy compression stages (ECSs) are used in SOS generators with an output energy of > 1 J. The efficiency of this approach is about 40 % due to losses in ECSs. Higher efficiency of up to 70 % can be reached using a single ECS such as a saturating pulse transformer [4].

Although in this case, a primary gas-discharge switch is required, which brings the aforementioned disadvantages into the system.

In this work, we propose a new single ECS circuit for pumping semiconductor opening switches such as DSRD and SOS diodes. The circuit is based on a vector inversion generator [5], also known as a spiral generator [6], which represents a double spiral-shaped stripline with a low-inductive primary switch. Using a low-voltage switch, the spiral generator can produce pulses of 100s kV due to the generous voltage multiplication factor, which depends on the coil turn number. The wave nature of a spiral generator is responsible for the non-symmetrical oscillations of the output voltage. The period of these oscillations can be in the submicrosecond range, depending on geometry. A combination of these factors makes the spiral generator an ideal circuit for pumping semiconductor opening switches.

Thanks to the advantages of modern semiconductor technology, an all-solid-state spiral generator [7] has been tested in this work as a prototype of the SOS diode pumping circuit. A spark gap, traditionally used in the spiral generator, was replaced by highly interdigitated thyristors [8] that are commercially available under the Solidtron brand [9].

The proposed approach can be used in pulsed power applications such as dielectric barrier discharge plasma sources [10], runaway electron research [11], and x-ray generation [12]. Also, this includes triggering the multichannel spark gap [13], impact-ionization thyristor driver [14], as well as pumping of the opening switch based on standard diodes, which has been reported in our previous work [15].

The paper is organized as follows. Section II describes the experimental setup, including the spiral generator, SOS diodes, and diagnostics. Section III shows the results of a generator prototype operating with resistive and capacitive loads. The conclusion summarizes the results obtained and suggests a path for future research.

II. Experimental Arrangement

A. Spiral Generator

As the main workhorse of this study, the spiral generator (SG) deserves a proper description. Schematically SG consists of three main components as shown in Fig. 1: spiral stripline, driver board DB, and switch Sw. The spiral stripline is initially charged up to 5 kV by the power supply installed in DB. After receiving an optical trigger pulse, DB turns on the switch Sw, starting the wave process in the spiral stripline. Eventually, this causes high voltage oscillations on the load connected to the high voltage output terminal HV. A detailed analysis of this SG as well as a description of its components can be found in [6] and [7].

Although the fabrication process was thoroughly explained in [7], here we need to describe the geometry of the spiral stripline since it determines the output pulse shape. The spiral in the present study has 24 turns, which form a bobbin with a total height of 75 mm, outer diameter of 60 mm, and inner diameter of 20 mm. Each layer is made from 50 mm copper tape 30 μm thick, laminated onto 75 mm Mylar strip, 250 μm thick. For this configuration, the spiral capacitance Cs is 17 nF. The spiral insulation is made by vacuum impregnation with epoxy resin. Tests at 5 kV revealed no flashover between layers of the spiral. Having a mean winding diameter of 40 mm and a conductive part width of 50 mm, this particular spiral generator is referred to as SG-40/50.

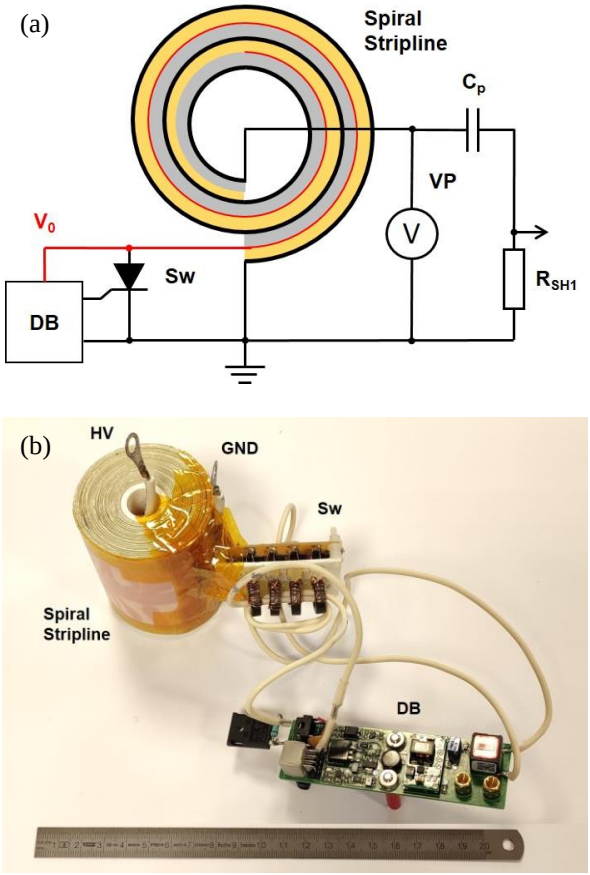

Fig. 1. Circuit diagram of the SG-40/50 spiral generator (a) and its appearance (b): Spiral Stripline – spiral pulse forming line, DB – driver board, Sw – solid-state switch, VP – voltage probe Tektronix P6015A, C_P – pumping capacitor, R_{SH1} – resistive shunt.

The input switch (Sw in Fig. 1) consists of four series-connected SP205-01 thyristors, also known as "Solidtrons" [9]. As it is customary when semiconductor items are connected in series, to equalize the voltage distribution each thyristor has a resistor of 100 MΩ (2512 package) connected in parallel. High voltage, high dI/dt, and low inductance are the distinguishing features of this solid-state switch, which are required for the proper operation of the spiral generator.

The switch Sw is controlled via four ferrite-based transformers (not shown in Fig. 1), which provide galvanic insulation and synchronization. The triggering pulse is formed by the control unit (DB in Fig. 1), which is driven by an external optical signal. Feeding this triggering pulse to the primary winding, common to all 4 ferrite-based transformers, allows to generate simultaneous pulses on the secondary windings, which are connected to the gate electrodes of the

SP205-01 thyristors. A detailed description of Sw and DB is provided in [7]. In addition, the DB carries a 5 kV regulated power supply to charge the spiral and an interlock to protect the user.

To verify the ability of the SG-40/50 to generate the current pulse required to pump the semiconductor opening switch, a pumping capacitor C_P was installed as shown in Fig. 1(a). High-voltage ceramic capacitors with a capacitance from 80 pF to 500 pF were tested. Looking at Fig. 2(a), one can find that the current shape is very similar to the typical currents of the SOS or DSRD diodes. In particular, it is an asymmetric sine of sub-microsecond duration, with the first half-period having a lower amplitude than the second half-period. This promising observation served as the motivation for this study.

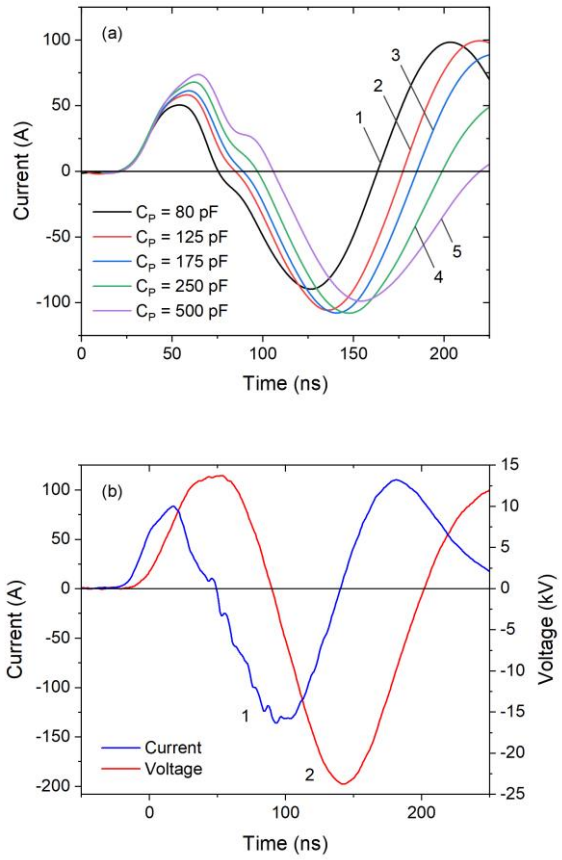

Fig. 2. The output current of the SG-40/50 with the different capacitive load C_P (a): 1 – 80 pF, 2 – 125 pF, 3 – 175 pF, 4 – 250 pF, 5 – 500 pF. The voltage across the C_P (1) and current of the SG-40/50 (2) at C_P=175 pF (b).

We choose a negative current amplitude as an optimization parameter because this current can be stored in an inductive energy storage and interrupted by a semiconductor opening switch. Analysis of the currents presented in Fig. 2(a) reveals the optimum value of C_P, which ranges approximately from 125 pF to 250 pF. The voltage across the pumping capacitor C_P = 175 pF and current through it are shown in Fig. 2(b).

For the capacitance of the spiral C_S = 17 nF, the stored electrostatic energy at a charging voltage V_0 = 4.7 kV is $W_S = C_S * V_0^2 / 2$ = 188 mJ. When the spiral generator is connected to a capacitive load C_P = 175 pF, the maximum load voltage generated is 23 kV (Fig. 2(b)), which corresponds to an energy W_C of 46 mJ. The overall energy efficiency Wc/Ws is therefore 25 %.

The voltage across the load is measured by the Tektronix P6015A voltage probe (VP in Fig. 1(a)). The current is measured by the in-house made current shunt R_{SH1} with a resistance of 0.48 Ω and usable rise time of 0.5 ns. The signal from R_{SH1} is captured with the Tectronix TDS7704B oscilloscope, using the Barth 142 attenuator (26 dB, 30 GHz). The same diagnostic techniques are employed in all further experiments.

B. Semiconductor Opening Switch

Two types of SOS diodes were provided by the Institute of Electrophysics, Russia. A diode blocking voltage is about 3 kV for both types and wafer areas are 1 cm² and 0.25 cm², respectively. The recommended maximum parameters of operation are as follows: forward current density 0.8 kA/cm², forward pumping time 500 ns, reverse current density 4 kA/cm², reverse pumping time 100 ns.

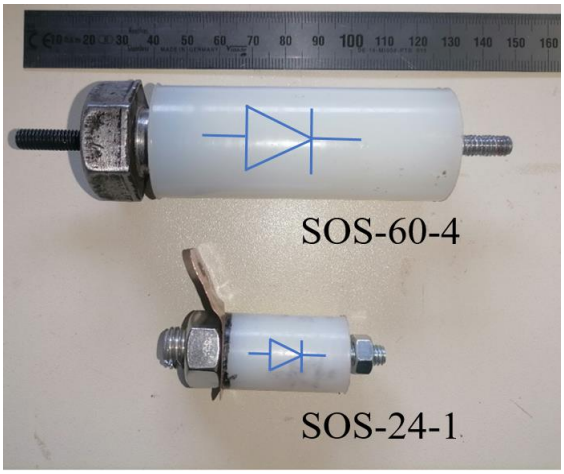

Fig. 3. Stack of 20 diodes with an area of 1 cm² connected in series – SOS-60-4 (top); stack of 8 diodes with an area of 0.25 cm² connected in series – SOS-24-1 (bottom).

To assemble SOS diodes in series, we developed two stacks, called SOS-60-4 and SOS-24-1, with a rated blocking voltage / reverse current of 60 kV / 4 kA and 24 kV / 1 kA, correspondingly. As shown in Fig. 3, the stack consists of an empty plastic tube in which the diodes are placed. The two opposite bolts serve as the clamping system as well as the cathode and anode terminals.

C. Spiral Generator Equipped with SOS Diodes

After the current shape was confirmed as suitable for SOS diodes, the SG-40/50 spiral generator was equipped with a stack of SOS diodes as shown in Fig. 4. The new generator was denoted as SG-SOS. The pumping capacitor C_P = 175 pF was chosen according to the optimization results. Currents through the load Z_{LOAD} and opening switch SOS connected in parallel are measured by two identical current shunts R_{SH1} and R_{SH2}. The load voltage can be measured by two independent

methods: (i) direct measurement by the voltage probe VP and (ii) a calculation based on Ohm's law, using the load current and load resistance. Another diode (not shown in Fig. 4) can be installed between the SOS and Z_{LOAD} to prevent diverting the SOS pumping current to a low-impedance load.

Let us describe the operation of the SG-SOS generator, using the configuration with SOS-60-4 and 1 kΩ resistive load as an example. Initially, the active layer of the spiral is charged to V_0 = 4.7 kV (Fig. 4). Turning on the Sw initiates the wave processes in the spiral. First, this results in the forward SOS current (Fig. 5, curve 1), which "pumps" the diode structure with electron-hole plasma. The reverse SOS current then causes a fast current cutoff, and the diode switches current to the load within a few ns (Fig. 5, curve 2). Finally, a high-voltage nanosecond pulse is formed across the load (Fig. 5, curve 3).

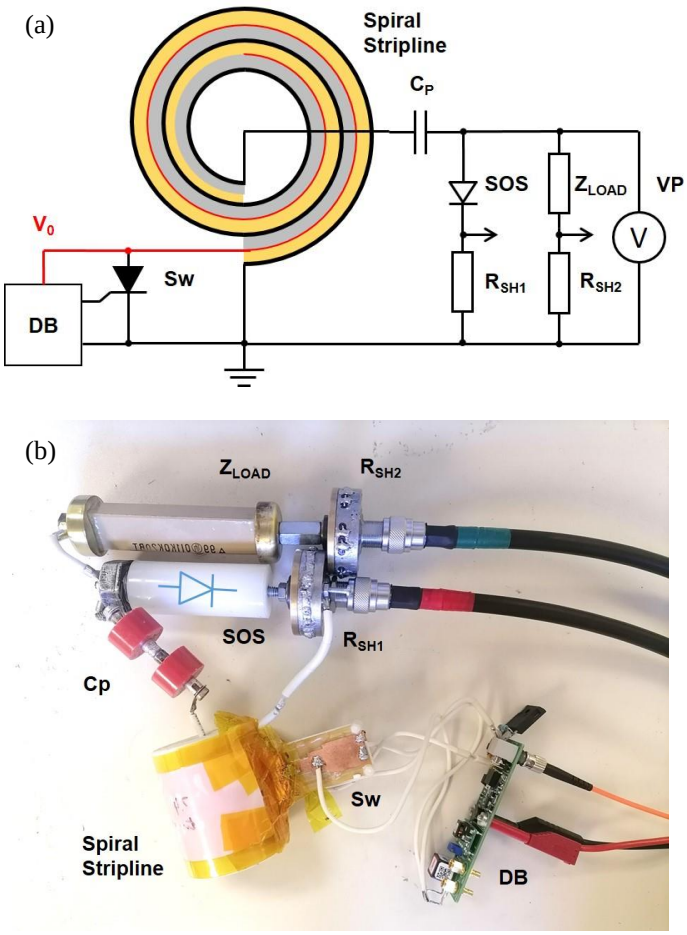

Fig. 4. Circuit diagram of the SG-SOS generator (a) and its configuration based on SOS-60-4 and Z_{LOAD} = 1 kΩ (b): Spiral Stripline – spiral pulse forming line, DB – driver board, Sw – solid-state switch, Cp – pumping capacitor, SOS – semiconductor opening switch, Z_{LOAD} – resistive or capacitive load, VP – voltage probe, R_{SH1} and R_{SH2} – resistive shunts.

According to Fig. 5 (curve 1), the SOS pumping current has the following parameters: forward amplitude I^+ = 56 A, forward pumping time t^+ = 58 ns, reverse amplitude I^- = 77 A, and reverse pumping time t^- = 38 ns. Corresponding reverse current density j^- = 77 A/cm² makes us believe that the opening switch operates rather in DSRD mode than SOS. The short switching time (6 ns) – typical for the DSRD mechanism – confirms this hypothesis. However, this has no negative effect on the load voltage, which has a rise time of 13 ns (0.1-0.9), amplitude of 41 kV, and duration of 29 ns (full width at half maximum – FWHM).

For the 1 kΩ resistive load, a load energy W_L = 36 mJ can be estimated from the load current and voltage (see Fig. 5, waveforms 2 and 3). This corresponds to a total efficiency of about 20 %, calculated as W_L / W_S for the spiral generator equipped with the SOS-60-4 diode.

We can see that the SOS diode can be driven by a spiral generator, delivering a high-voltage pulse into the resistive load. Operation at different loads will be discussed in the next section.

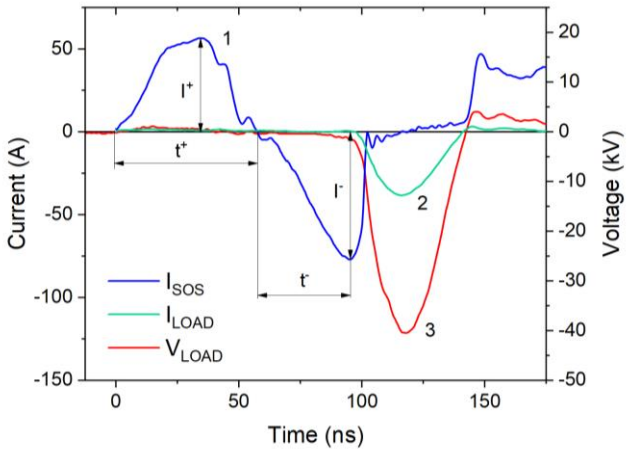

Fig. 5. Typical waveforms of the SOS-60-4 diode current (1), load current (2), and load voltage (3) at the 1 kΩ resistive load.

III. Load Characteristic

A. Resistive Load

In this section, two resistive loads tested with two SOS diodes, as shown in Fig. 4, are discussed. The first 1 MΩ load is simply represented by the voltage probe Tektronix P6015A (VP in Fig. 4), which has a resistance of 1 MΩ and parasitic capacitance of 3 pF according to the datasheet. We consider this as an open circuit load, where the maximum voltage amplitude is obtained. For the second 325 Ω load, carbon composition resistors were employed (Z_{LOAD} in Fig. 4). A value of 325 Ω was chosen to compare the SOS-60-4 and SOS-24-1 diodes, as they can both withstand the voltage that arises at this load. The waveforms of the SOS current and load voltage are summarized in Fig. 6.

When the load voltage tends to exceed the SOS diode rating, the diode limits the voltage by conducting current. This situation is observed for SOS-24-1 operated at 1 MΩ load in Fig. 6(a). As can be seen, the SOS current (Fig. 6(a), curve 1) rises sharply when the voltage across the load and diode reaches 25 kV (Fig. 6(a), curve 2), which is close to the nominal voltage for SOS-24-1. It leads to a quasi-square pulse

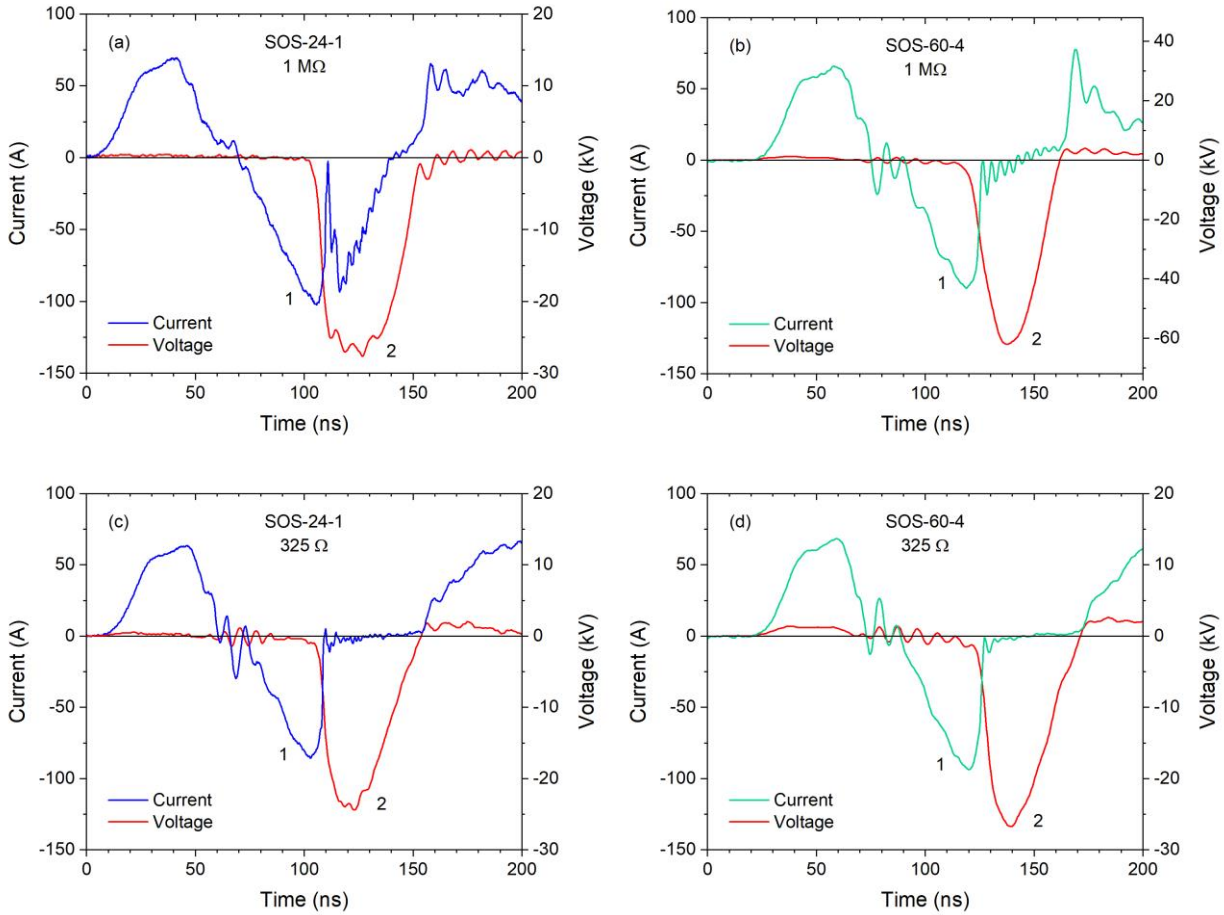

Fig. 6. Typical waveforms of the SOS current (curve 1) and load voltage (curve 2) obtained with SOS-24-1 at 1 MΩ (a) and 325 Ω (c), and SOS-60-4 at 1 MΩ (b) and 325 Ω (d).

across the load with a flat top part determined by the duration of the current delivered by the pumping circuit. For SG-40/50, the flat top duration is about 25 ns. However, the diode remains intact as long as the pulse duration is shorter than the critical value, which is determined by the power dissipation during the conductive state at the high voltage (between 110 ns and 140 ns in Fig. 6(a)). Longer pulses lead to more energy being deposited in the semiconductor structure, which may cause an irreversible thermal breakdown. The time and the corresponding critical energy are usually found empirically, by trial and error. The observed effect may be used in the design of square pulse generators.

The SOS-60-4 diode allows obtaining up to 62 kV at 1 MΩ resistive load (Fig. 6(b), curve 2). It can be observed that there is no current through the diode after the cut-off (Fig. 6(b), curve 2), which does not form a flat top voltage on the load. As shown in Fig. 6(c) and Fig.6(d), reducing the load to 325 Ω makes the SOS-24-1 and SOS-60-4 operate identically because the load voltage is below the rated value.

The summary of the load voltage and diode current parameters is presented in Table I. Changing load resistance from 325 Ω to 1 MΩ weakly affects the diode current shape. Thus, the diode pumping parameters provided by the spiral generator remain almost constant: $t^+ \approx 65$ ns, $I^+ \approx 66$ A, $t^- \approx 36$ ns, and $I^- \approx 93$ A. Although further decreasing of the load resistance will affect the current shape, SG-SOS operation with, for instance, 50 Ω is possible. This requires an isolating element, such as a capacitor or diode, to prevent redirection of the diode pumping current to the load.

The load energy in Table I was calculated using the voltage amplitude and load capacitance for the 1 MΩ load, which gives approximate values. For the 325 Ω load, directly measured load current and voltage give more accurate results. An efficiency of 0.25 can be calculated in this case, using the method described in Section II.

TABLE I
LOAD VOLTAGE AND SOS CURRENT PULSE PARAMETERS OBTAINED WITH A RESISTIVE LOAD

Parameter	1 MΩ (3 pF)		325 Ω	
Diode type	SOS-24-1	SOS-60-4	SOS-24-1	SOS-60-4
Voltage, kV	26	62	24	27
Rise time, ns	5	11	8	10
FWHM, ns	37	27	30	28
Energy, mJ	~1	~6	40	47
t^+, ns	70	70	60	60
I^+, A	70	65	63	68
t^-, ns	35	35	35	40
I^-, A	102	90	84	94

B. Capacitive Load

Low-inductance, high-voltage ceramic capacitors in various combinations were used to test SG-SOS loaded to the capacitive load Z_{LOAD} according to the circuit shown in Fig. 4(a). The pumping capacitor was set to C_P = 125 pF and the SOS-24-1 diode was tested. Typical waveforms of the voltage across the load for the load capacitance ranging from 20 to 130 pF are presented in Fig. 7(a). Voltage magnitude and load energy as a function of the load capacitance are plotted in Fig. 7(b). Table II summarizes the voltage pulse parameters.

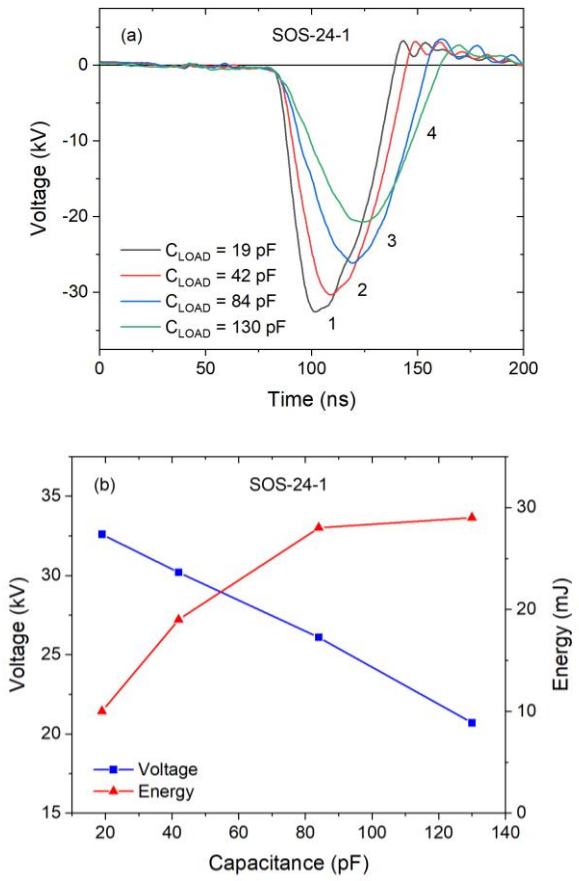

Fig. 7. Waveforms of the voltage across the capacitive load (a) and voltage amplitude (square) and load energy (triangle) as a function of load capacitance (b) for the SOS-24-1 diode.

As can be seen in Fig. 6(a), the voltage limit of the SOS-24-1 diode is about 25 kV in open circuit operation (1 MΩ, 3 pF). However, as shown in Fig. 7(a), a voltage of 33 kV can be obtained using the same diode with a 19 pF capacitive load. This voltage was verified by two independent measurement techniques: (i) by the voltage probe Tektronix P6015A and (ii) by the ratio of the charge to capacitance, where the charge was calculated as a time-integral of the load current. The higher voltage generated across the capacitive load can be explained by carefully analyzing the electromagnetic characteristics of the connection between the generator and a capacitive load. In such a case, the parasitic inductance between the SOS diode and the load stores magnetic energy during the application of the current impulse. Later, this energy is delivered to the load after the SOS diode returns to the conductive state when its breakdown voltage is reached. This leads to the load voltage exceeding the rated voltage of the SOS diodes. This unwanted phenomenon was (qualitatively) confirmed by PSpice circuit analysis.

TABLE II
PARAMETERS OF THE VOLTAGE PULSE ACROSS THE CAPACITIVE LOAD FOR THE SOS-24-1 DIODE

Parameter	SOS-24-1			
Capacitance, pF	19	42	84	130
Voltage, kV	33	30	26	21
Rise time, ns	12	15	23	29
FWHM, ns	37	39	44	47
Energy, mJ	10	19	28	29

It has been observed that the SOS-24-1 diode limits the load voltage at an amplitude of about 25 kV, which is the nominal voltage of this diode. This can be seen as a change in the slope of the curve with a bend point of about 25 kV in Fig. 7(b). The current flowing through the diode at voltages above 25 kV also confirms this limitation. A similar effect is observed for the resistive 1 MΩ load (Fig. 6(a)). When installing the SOS-60-4 diode, a voltage pulse with an amplitude of 39 kV, rise time of 19 ns, and FWHM of 36 ns was obtained at 19 pF.

The energy delivered into the capacitive load (Table II) was calculated using the load capacitance and voltage amplitude. The efficiency increases with the capacitance value, reaching 0.15 at the 130 pF load. A load with a higher capacitance was not tested in this work because it required an additional component to decouple the SOS diode from the low-impedance load during pumping.

We believe that the overall efficiency of SG-SOS generators can be increased by matching the output impedance to the load. The use of an additional inductor may be a solution, however, its effect on the spiral generator must be tested.

V. CONCLUSION

To the best of the authors' knowledge, this work is the first attempt to use a spiral generator as a pumping circuit for a semiconductor opening switch. An all-solid-state spiral generator equipped with SOS diodes has been tested on resistive and capacitive loads, with efficiencies of 20 % for 1 kΩ resistive load and 15 % for 19 pF capacitive load. A voltage pulse with a peak of 62 kV, rise time of 11 ns, and duration of 27 ns was successfully generated on an open circuit (1 MΩ, 3 pF) when a current of about 65 A was cut off by the SOS. The results were highly reproducible and there was no degradation in the performance of the generator components during all tests (more than 100 shots). Promising results justify the proposed approach and encourage further research. Despite the lack of adjustability and relatively low efficiency of a spiral generator, this approach is a cost-effective way to build compact solid-state generators of high-

voltage nanosecond pulses. Further research can be focused on more energetic versions, which require modification of the spiral and the primary switch. Being adjusted to a specific load, these generators can be employed in numerous pulsed power applications, such as impact ionization switches, multi-channel spark gaps, plasma-activated water, and others. In addition, testing a spiral generator as a pumping circuit for the off-the-shelf diodes is of great interest, since it would significantly reduce the cost of nanosecond pulse generators, making them available to a broad range of researchers.

ACKNOWLEDGMENT

The authors express their gratitude to Dr. Rukin (Institute of Electrophysics, Russia) for providing the SOS diodes for testing.

REFERENCES

[1] I. V. Grekhov, V. M. Efanov, A. F. Kardo-Sysoev, and S. V. Shenderey, "Power drift step recovery diodes (DSRD)," *Solid. State. Electron.*, vol. 28, no. 6, pp. 597–599, Jun. 1985.

[2] Y. A. Kotov, G. A. Mesyats, S. N. Rukin, A. L. Filatov, and S. K. Lyubutin, "Novel nanosecond semiconductor opening switch for megavolt repetitive pulsed power technology: Experiment and applications," *IEEE Int. Pulsed Power Conf. - Dig. Tech. Pap.*, vol. 1, pp. 134–139, 1993.

[3] I. V Grekhov and G. A. Mesyats, "Nanosecond semiconductor diodes for pulsed power switching," *Physics-Uspekhi*, vol. 48, no. 7, pp. 703–712, Jul. 2005.

[4] S. N. Rukin, "Pulsed power technology based on semiconductor opening switches: A review," *Rev. Sci. Instrum.*, vol. 91, no. 1, p. 011501, Jan. 2020.

[5] R. A. Fitch and V. T. S. Howell, "Novel principle of transient high-voltage generation," in *IEE Science and general*, 1964, vol. 111, pp. 849–855.

[6] J. Yan, S. Parker, and S. Bland, "An Investigation Into High-Voltage Spiral Generators Utilizing Thyristor Input Switches," *IEEE Trans. Power Electron.*, vol. 36, no. 9, pp. 10005–10019, Sep. 2021.

[7] J. Yan, S. Parker, T. Gheorghiu, N. Schwartz, S. Theocharous, and S. N. Bland, "Miniature solid-state switched spiral generator for the cost effective, programmable triggering of large scale pulsed power accelerators," *Phys. Rev. Accel. Beams*, vol. 24, no. 3, p. 030401, Mar. 2021.

[8] H. Sanders and J. Waldron, "Tailoring high-voltage, high-current thyristors for very high frequency switching," in *2016 IEEE International Power Modulator and High Voltage Conference (IPMHVC)*, 2016, no. May, pp. 179–182.

[9] "Solidtron | Excelitas." [Online]. Available: https://www.excelitas.com/product-category/solidtron. [Accessed: 11-Dec-2022].

[10] K. Takashima and T. Kaneko, "Ozone and dinitrogen monoxide production in atmospheric pressure air dielectric barrier discharge plasma effluent generated by nanosecond pulse superimposed alternating current voltage," *Plasma Sources Sci. Technol.*, vol. 26, no. 6, p. 065018, Jun. 2017.

[11] B. Huang, C. Zhang, C. Ren, and T. Shao, "Guiding effect of runaway electrons in atmospheric pressure nanosecond pulsed discharge: mode transition from diffuse discharge to streamer," *Plasma Sources Sci. Technol.*, vol. 31, no. 11, p. 114002, Nov. 2022.

[12] B. Huang, C. Zhang, J. Qiu, X. Zhang, Y. Ding, and T. Shao, "The dynamics of discharge propagation and x-ray generation in nanosecond pulsed fast ionisation wave in 5 mbar nitrogen," *Plasma Sources Sci. Technol.*, vol. 28, no. 9, p. 095001, Sep. 2019.

[13] A. A. Kim *et al.*, "Multi gap, multi channel spark switches," in *Digest of Technical Papers. 11th IEEE International Pulsed Power Conference (Cat. No.97CH36127)*, 1997, vol. 2, pp. 862–867.

[14] A. I. Gusev, S. K. Lyubutin, S. N. Rukin, and S. N. Tsyranov, "Superfast Thyristor-Based Switches Operating in Impact-Ionization Wave Mode," *IEEE Trans. Plasma Sci.*, vol. 44, no. 10, pp. 1888–1893, Oct. 2016.

[15] M. R. Degnon *et al.*, "Off-the-Shelf Diodes as High-Voltage Opening Switches," *IEEE Trans. Plasma Sci.*, vol. 50, no. 10, pp. 3384–3392, 2022.